Magazine of Civil Engineering

ISSN 2712-8172

journal homepage: http://engstroy.spbstu.ru/

Research article

UDC 639.42:539.42

DOI: 10.34910/MCE.132.3

Electrically conductive cement composites modified with weakly oxidized graphene

E.D. Vasileva[1] ✉ , ***D.N. Popov***[1,2] , ***P.V. Vinokurov***[3] , ***A.L. Popov***[4]

[1] *North-Eastern Federal University, Yakutsk, Russian Federation*

[2] *V.P. Larionov Institute of the Physical-Technical Problems of the North of the Siberian Branch of the RAS, Yakutsk, Russian Federation*

[3] *North-Eastern Federal University in Yakutsk, Yakutsk, Russian Federation*

[4] *Institute of problems of oil and gas of the Siberian Branch of the Russian Academy of Sciences, Yakutsk, Russian Federation*

✉ *vasilyeva_edm@mail.ru*

Keywords: Concrete, cements, compressive strength, Portland cement, composite materials, multi-layer graphene oxide, cement composite, dispersion, self-diagnostics.

Abstract. This study investigates the influence of graphene on the electrical conductivity and mechanical properties of concrete composites, aiming to develop advanced materials for structural applications. Graphene's exceptional electrical conductivity can significantly enhance inert concrete matrices by forming a conductive network. Concrete samples were prepared with minimally oxidized graphene (MOG) at 0.2 and 0.5 % by weight of cement. Spectroscopic techniques, including Raman and infrared spectroscopy, were employed to characterize the interaction between graphene and the cement matrix. Results showed that the addition of MOG reduced electrical resistivity, with the 0.2 % sample decreasing from approximately 600 to 550 Ohm under compression. The yield point was around 40–50 kN, with a sharp decline in resistivity at this load. Compressive strength tests indicated a 48 % increase in strength with just 0.05 % graphene oxide. These findings suggest that graphene incorporation enhances both electrical conductivity and mechanical strength, making the composites suitable for applications in structural health monitoring and self-heating systems.

Funding: This study was supported by the Russian Science Foundation (project No. 24-21-20122).

Citation: Vasileva, E.D., Popov, D.N., Vinokurov, P.V., Popov, A.L. Electrically conductive cement composites modified with weakly oxidized graphene. Magazine of Civil Engineering. 2024. 17(8). Article no. 13203. DOI: 10.34910/MCE.132.3

1. Introduction

It is known that graphene has the highest electrical conductivity among known materials [1–4]. The addition of even a small amount of graphene can significantly increase the electrical conductivity of an initially inert dielectric concrete matrix due to the formation of a conductive network. A few works by authors, such as Sassani, Wang, Choi, Ghosh et al. [5–21, 26], are devoted to the study of the electrical properties of cement composites with the addition of graphene and graphene oxide, which show a sharp increase in electrical conductivity and the appearance of pronounced piezoresistive effects. The prospects for using such composites as self-sensing "smart" materials are discussed [27]. Such electrically conductive cement composites can be used in systems for heating road surfaces and airfields instead of traditional methods of removing ice and snow using chemicals. At the same time, in the study [7], the authors identified

problems with the stability of electrical conductivity and energy consumption of heating systems based on carbon-cement composites during long-term operation.

The group of researchers [11–16] focused on studying the mechanical properties of graphene-cement composites. The addition of a small amount, from 0.1 to 1 %, by volume of carbon nanoparticles leads to a sharp increase in the electrical conductivity of cement composites by several orders of magnitude. Which is associated with the formation of a continuous conductive network through the cement matrix and also allows significantly improving the mechanical characteristics of cement composites by increasing compressive, tensile and flexural strength.

In the review works of Nochaiya and Schulte [17–18], the results of studies of graphene-cement composites are summarized, and the current state and application prospects in construction are analyzed. Various methods of dispersing graphene in a cement matrix are considered in detail – ultrasonic treatment, use of surfactants, and functionalization of graphene to improve wettability. The importance of obtaining a homogeneous and stable dispersion of graphene is shown.

Rostami [11] investigated the microstructure of composites using SEM, FTIR, XRD, TGA and revealed the effect of graphene on particle packing density, porosity reduction, change in hydrate composition, and acceleration of hydration processes. In the work of Li [20], an original approach is proposed for growing graphene directly on the surface of aggregates. This improves adhesion to the cement matrix while simultaneously imparting electrical conductivity.

The addition of carbon nanomaterials also improves the thermoelectric properties of cement composites by increasing the Seebeck coefficient [8–10, 14, 18, 24], which opens up ways for creating thermoelectric generators based on cement. Of particular interest are hybrid systems combining, for example, graphene and metal oxides, which make it possible to simultaneously increase electrical conductivity and the Seebeck coefficient. Oxidation of graphene improves its dispersion and adhesion to the cement matrix due to the formation of polar groups.

Du et al. and Konsta-Gdoutos [21–23, 4] considered the problem of the aggregation of graphene particles in the cement matrix, leading to heterogeneity and a decrease in the reinforcing effect. Solutions are proposed – the use of functionalized graphene as well as the application of graphene to the surface of aggregates.

For creating electrically conductive concretes, the selection of conductive additives is important, and for improving the stability and sensitivity of electrical characteristics to mechanical influences, the development of special composite concretes is required. Although the potential of graphene as a functional additive is very promising, the use of graphene concretes as “smart” materials for self-diagnostics is still at the research stage. The relevance of the work is due to the prospects for using such composites as self-sensing structural materials capable of monitoring stresses and strains during operation. This will improve the operational reliability and durability of concrete structures.

The aim of the work is to study the effect of graphene on the electrical conductivity of concrete composites, to determine the change in strength due to the inclusion of graphene, as well as to assess the potential for the use of graphene-modified concrete in various fields of mechanical engineering.

2. Methods

2.1. Spectroscopic Analysis and Microscopy

Raman spectroscopy, combined with atomic force microscopy (AFM) and confocal Raman/fluorescence microscopy and spectroscopy using the NTEGRA Spectra system, was employed to detect and identify graphene in concrete. This method allowed for the revelation of the interaction between graphene particles and the surrounding concrete matrix. Additionally, microphotographs and elemental analysis of the concrete surfaces were obtained using a scanning electron microscope (SEM) equipped with an EDS-WDS microanalysis system (JSM 6480LV INCA Energy 350, JEOL Ltd, Oxford Instruments, Japan, UK).

2.2. Preparation of Graphene-Modified Concrete

To experimentally confirm the use of an aqueous suspension of minimally oxidized graphene (MOG), obtained by electrochemical exfoliation of graphene as described in [28]. Minimally oxidized graphene (MOG) was obtained by electrochemical exfoliation in a 1.42 % aqueous sodium sulfate solution (Na_2SO_4). Two electrodes were used for this method: a gold electrode (6 mm wide and 0.015 mm thick) and a graphite electrode (ESA-16 grade with a diameter of 6 mm). The gold electrode acts as a cathode, and the graphite electrode acts as an anode. Both electrodes were immersed in 200 ml electrolyte to a depth of 60 mm, and the distance between them was 20 mm (Fig. 1, a). At a voltage of 12 V, the graphite electrode was

exfoliated for 60 minutes (Fig. 1, b). Then, using an ultrasonic homogeniser Up 200St (Hielscher Ultrasonics, Germany), large carbon particles were split into MOGs.

a b

Figure 1. MOG synthesis: a – electrochemical exfoliation process; b – Electrochemical exfoliation process after 60 min.

As a binder for the concretes, Portland cement of the grade CEM I 32.5B, produced by AO PO “Yakutcement” in accordance with the interstate standard GOST 31108-2016, was used. River sand from the floodplain of the Lena River, corresponding to all characteristics of the group “very fine” in accordance with the interstate standard GOST 8736, was used as a fine aggregate in the concrete. Crushed stone from a mixture of fractions from 10 to 40 mm, produced by AO PO “Yakutcement” from limestone rocks in the village of Mokhsogollokh in accordance with the interstate standard GOST 8267-93, was used as a coarse aggregate.

As a plasticizing admixture for the concretes in this work, a highly concentrated superplasticizing admixture based on polyaryl and polycarboxylate ethers for concretes with enhanced retainability – MasterPolyheed 4001 to decrease retardation effects on cement hydration [29], in accordance with the organizational standard STO 70386662-309-2021, is used. The working composition of the concrete was adopted as the composition selected according to GOST 27006-2019 for the chosen materials for the normative strength corresponding to class B12.5 in accordance with the interstate standard GOST 26633-2015. The initial components, shown in Table 1, were mixed using an LS-CB-10 laboratory mixer and compacted in molds measuring 100 × 100 × 400 mm using a VM-6.4 vibration table, following interstate standard GOST 10180-2012. The weighing of the components was performed on A&D GF-6100 electronic scales. The concretes was prepared in the “Building Materials” laboratory of the Engineering and Technical Institute of NEFU (Yakutsk, Russia).

Table 1. Composition of the concrete mix.

Composition	Mass, kg
Portland cement CEM I 32,5	5.62
Limestone aggregate 10–20 and 20–40 mm	16.16
Water	2.76
River sand	7.73
Plasticizer + liquid glass	0.114
Reduced oxidized graphene (MOG) 0.2 и 0.5 %	0.011 и 0.031

2.3. Electrical Resistivity Measurements

To measure the resistivity of concretes in a free state, a digital multimeter FAZA MAS830L (Russia) was used. The specific resistivity of concrete during loading was measured using a programmable power supply AKTAKOM APS-7151 (Finland). For this purpose, 4 mesh electrodes made of stainless steel, sized 8 × 12 cm, were embedded into the samples in the form of prisms measuring 40 × 10 × 10 cm during molding. Analysis of the behavior of the electrical resistivity of concrete under deformation was carried out according to interstate standard GOST 10180-2012.

2.4. Mechanical Testing

The concrete samples were tested for compression on a hydraulic press IP-1250M-auto (Russia) according to interstate standard GOST 10180-2012 (Fig. 2). The samples were loaded after 7, 14 and 28 days. The test was completed when a crack appeared on two sides of the sample.

Figure 2. Photo of mechanical testing and electrical resistivity measurements.

3. Results and Discussion

Based on the conducted Raman spectroscopy studies (Fig. 3) of concretes after 28 days with minimally oxidized graphene (MOG), the presence of hydroxyl groups (–OH) in the wavenumber range of 3200–3400 cm^{-1} enhances bonding within the cement matrix, reducing porosity and increasing resistance to water penetration [30]. Carbonyl groups (C=O), observed in the range of 1600–1800 cm^{-1}, participate in forming additional bonds, thereby improving the concrete's strength and chemical resistance [31]. Additionally, the presence of unsaturated carbon bonds (C=C) in the range of 1400–1600 cm^{-1} enhances flexibility and crack resistance, crucial for maintaining structural integrity [32].

Further modifications include the presence of C–H bonds, noted in the range of 2800–3000 cm^{-1} which are associated with organic components that reduce brittleness and improve resilience to mechanical stresses [33]. Peaks observed in the 2200–2400 cm^{-1} range suggest the presence of C≡C bonds or nitriles, indicating potential organic additives [34]. These functional groups collectively contribute to a denser microstructure, enhancing the material's overall durability and resistance to environmental degradation [35].

The unusual appearance of the red spectrum for MOG can be attributed to several factors. Structural heterogeneity in minimally oxidized graphene (MOG) leads to diverse spectral features, as different regions of the material interact variably with infrared radiation. Additionally, defects, such as vacancies or incomplete bonds in the graphene structure, cause scattering and anomalies, resulting in the spectrum's "unusual" appearance. Variations in oxidation levels influence the presence and intensity of functional groups like –OH and –COOH, creating complex spectra with multiple peaks [36].

The multilayered structure of MOG can induce complex vibrational modes, causing additional peaks and spectral anomalies in the intensity and line positions of moisture or other substances in the sample. These factors collectively contribute to the complexity of the MOG spectrum, reflecting its unique physical and chemical properties, and making interpretation challenging.

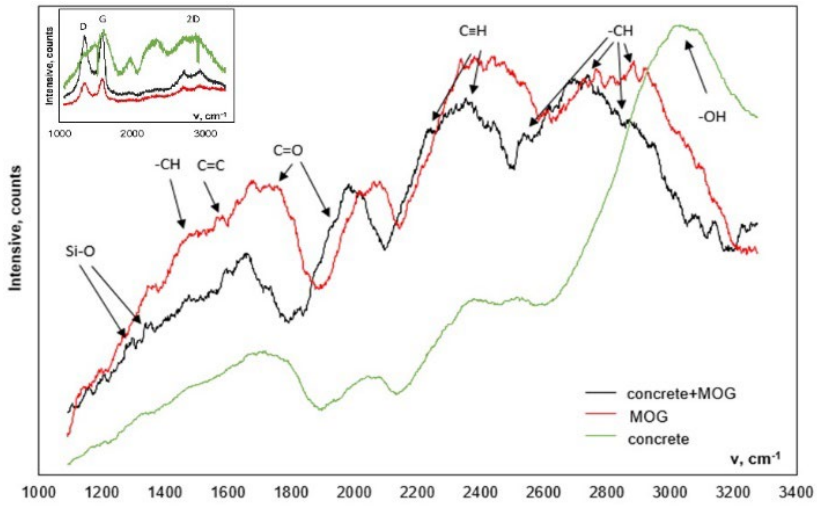

Figure 3. Raman spectrum of concrete modified with MOG after 28 days.

To reveal a more complete molecular picture of the concrete composition, an additional study was carried out by IR spectroscopy on an FTS 7000 IR Fourier step-scan spectrometer (Varian, USA) using an ATR attachment (Fig. 4).

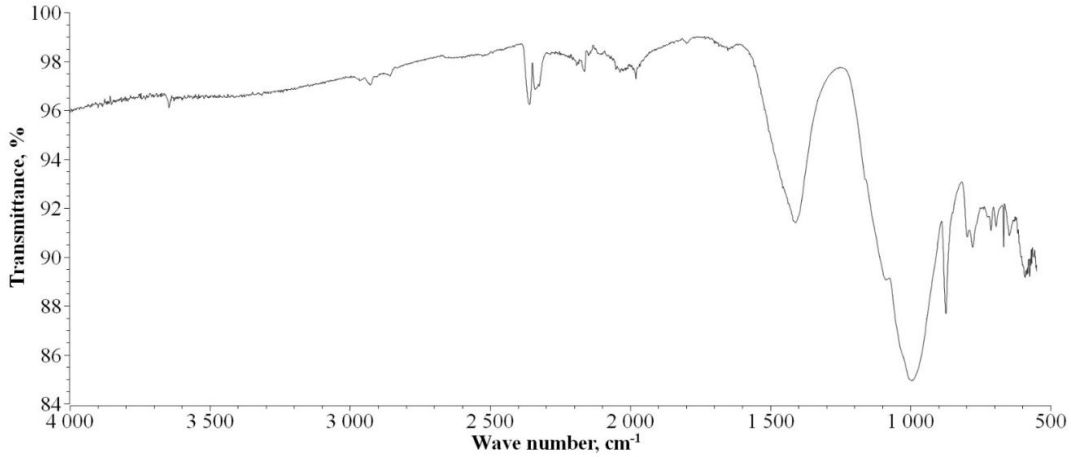

Figure 4. IR spectrum of concrete modified with MOG after 28 days.

From the IR spectrum of the concrete mix, the presence of organic impurities of polymer can be confirmed by the bands at 2930 and 2860 cm^{-1}, which may substantiate the hypothesis about the possible contribution of C–H vibrations to the peak at 2750 cm^{-1} in the Raman spectrum. The appearance of a peak at 2165 cm^{-1} from triple C≡C bonds is likely due to combination scattering on the triple C≡C bonds in graphene fragments. That is, this may be a characteristic peak of graphene itself, included in the composite material formulation. The intensity of this peak in the IR spectrum is usually low due to the selection rules for vibrations with an even number of atoms in the molecule. But nevertheless, it can be observed. The broad intense band at 1000 cm^{-1} and peaks in the 500–800 cm^{-1} region are due to vibrations of various mineral components of the cement stone.

Based on a comprehensive analysis of Raman and infrared spectra, it was found that the introduction of graphene is confirmed by the appearance of characteristic G (1600 cm^{-1}) and D (1350 cm^{-1}) peaks indicating the incorporation of graphene particles into an inert mineral matrix. The spectra were recorded using a laser at wavelengths of 633 and 514 nm. Signs of component interaction were detected – gas adsorption, possible functionalization of the graphene surface. The presence of additional organic impurities from the source materials was also revealed. In general, the study demonstrated the promise of the studied approach for evaluating the effectiveness of modifying concrete properties with carbon nanomaterials using a set of spectroscopic techniques.

According to the microphotographs (Fig. 5) of concrete, it can be seen that the concrete structure is heterogeneous, consisting of various phases and inclusions [37]. Both large inclusions up to 100 μm in size and smaller submicron particles are observed. The shape of the particles is predominantly rounded. From Table 2, the main elements are oxygen, silicon, carbon and calcium. This corresponds to the composition of cement stone based on calcium hydrosilicates and hydroaluminates. Mineral additives containing

sodium, magnesium, aluminum, sulfur, potassium and iron are also present. These are likely sand, ash and other fillers. The distribution of elements is quite uniform, no significant accumulations of any phases are observed. This indicates uniform mixing of components during concrete production. The absence of chlorine indicates the use of low-chloride cement, which has a positive effect on the corrosion resistance of concrete. By the carbon distribution, it can be assumed that there is no aggregation in the obtained samples, and the ratio of carbon to the total number of components exceeding 15–30 % indicates the sensitivity of the method for detecting MOG.

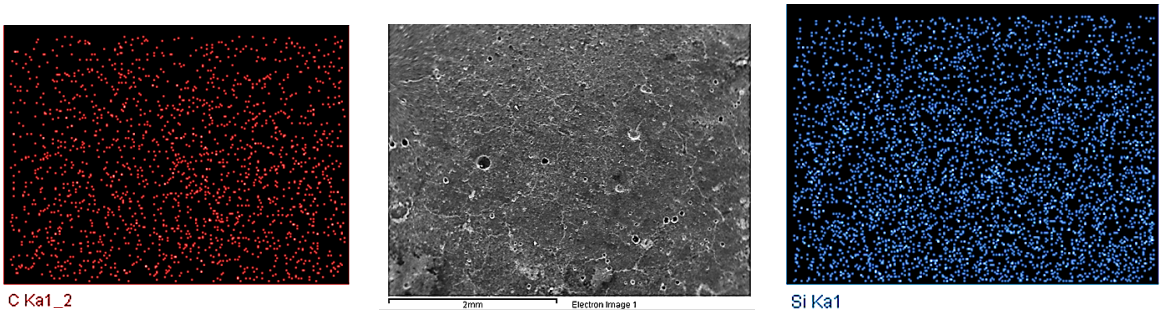

Figure 5. Microphotographs of the concrete 28 days surface showing the distribution of C and Si atoms.

Table 2. Distribution of components in the studied sample (Fig. 5).

Spectrum	C	Na	Mg	Al	Si	Cl	K	Ca	Fe	Total
Sum Spectrum	47.05	1.41	1.00	2.11	11.19	0.00	1.86	33.37	1.18	99.18
Mean	47.05	1.41	1.00	2.11	11.19	0.00	1.86	33.37	1.18	99.18
Std. deviation	0.00	0.00	0.00	0.00	0.00	0.00	0.00	0.00	0.00	–
Max.	47.05	1.41	1.00	2.11	11.19	0.00	1.86	33.37	1.18	–
Min.	47.05	1.41	1.00	2.11	11.19	0.00	1.86	33.37	1.18	–

*All results in compound, %

Figs. 6 and 7 show graphics of the compressive strength of concrete at different concentrations of MOG 7, 14 and 28 days and photographs of concrete samples after compression tests. The load applied to the concrete was calculated in kN per base area of the prism, equal to 10,000 mm^2. According to the test results of B12.5 grade concrete (strength up to 12.5–15.5 MPa) with 0.2 and 0.5 % MOG content by cement weight, it was revealed that when MOG is added to the concrete mix, the resistivity of the finished product decreases with increasing external load (compression). The rate of change in the resistivity of concrete decreased with increasing compression of the sample (Fig. 8). A sharp drop in resistivity when reaching the critical load level indicates high sensitivity to mechanical deformation. The yield point of concrete was observed in the range of 40–50 kN for all concrete ages.

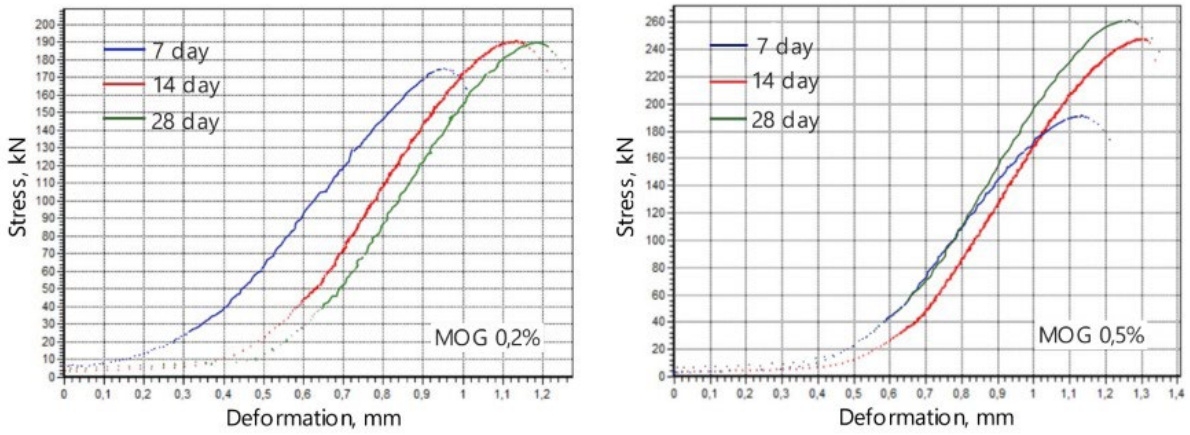

Figure 6. Compressive strength at different concentrations of MOG 7, 14 and 28 days.

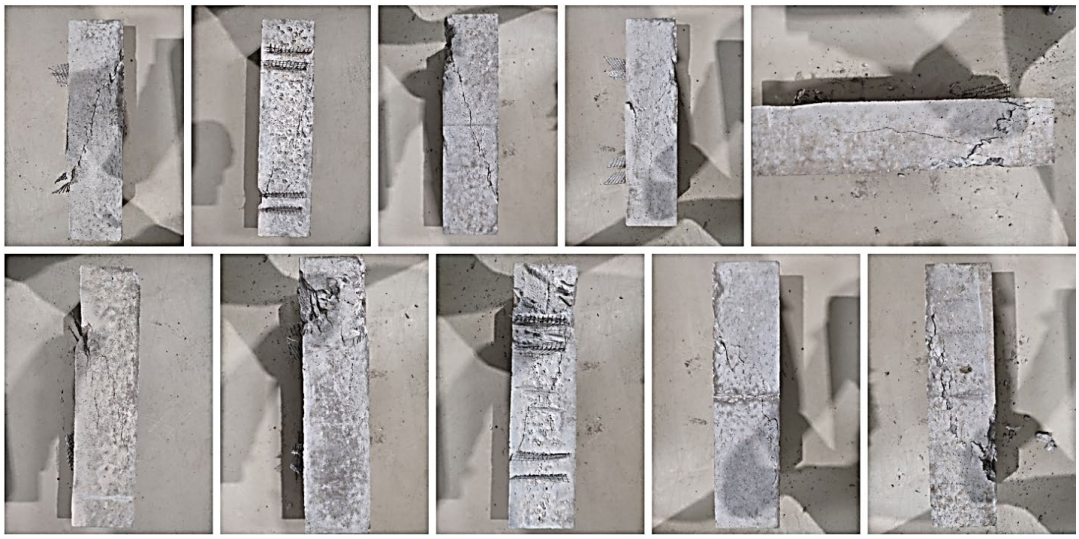

Figure 7. Photographs of modified concrete after testing.

The samples showed traces of vibration compaction in the concrete mixture due to molding. The nature of the destruction of the samples indicates brittle destruction without plastic deformation. The shape of the cracks allows us to estimate the stress-strain state of the samples during failure. The cracks propagate perpendicular to the direction of the applied compressive load, which corresponds to the laws of fracture mechanics of brittle materials. The absence of curved or inclined cracks indicates the isotropy of concrete properties in different directions. The clear, straight edges of the cracks indicate the brittle nature of destruction without plastic deformation. The relatively flat surface of the cracks without waviness or irregularities indicates a homogeneous concrete structure. The splitting of the sample into two parts along one plane confirms the brittle destruction under compressive load. The absence of spall, chips and delamination indicates sufficient strength of the aggregate bond with the cement stone. The color of the samples is uniform; no visible defects or delamination are observed.

The results obtained in this work on the mechanical properties of graphene oxide-modified cement composites are in agreement with previous studies. Pan et al. at work [38] reported an increase in compressive strength of 48 % with graphene oxide adding only 0.05 % to the weight of cement. Peng et al. at work [39] also showed that small additions of graphene oxide up to 0.05 % enhanced the flexural and compressive strengths of cement mortars.

The destruction of the concrete samples occurred from the side in contact with the plate until a crack reached the edge of the electrode sides (deformation). Thus, to measure the samples during loading, it is necessary to replace the 4-probe method with the 2-probe method, eliminating the influence of external factors on the stability of the resistivity value (material, conductive adhesive, drying rate of the adhesive, moisture content of the material itself).

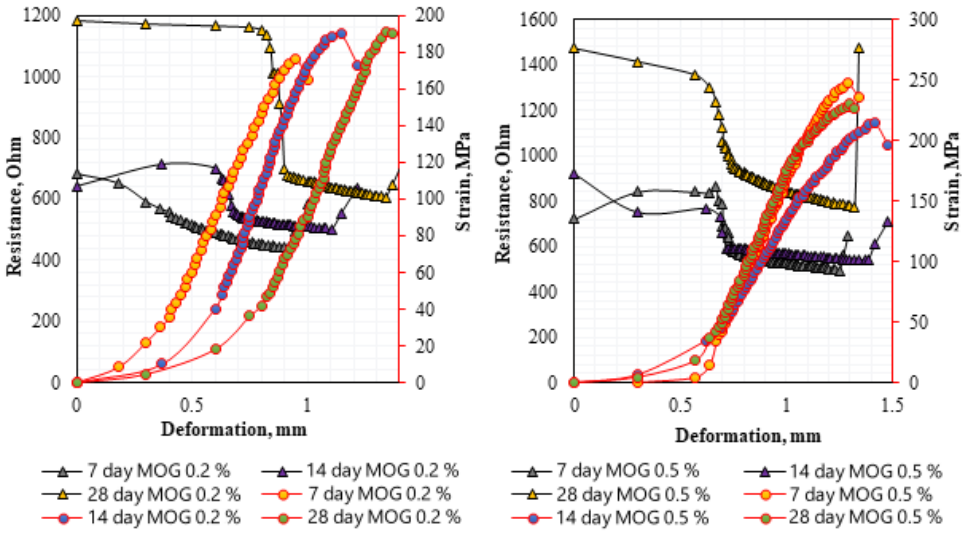

Figure 8. Graphs of the dependence of the change in the internal resistance of samples with 0.2 % MOG content (left) and 0.5 % MOG content (right) on deformation and load for 7, 14 and 28 days of curing.

Fig. 9 shows graphs of the dependence of the electrical resistivity of concrete samples on load. The electrical resistivity decreases with increasing load for all samples, which indicates the sensitivity of concrete to compression deformation. The electrical resistivity drops fastest at the beginning of loading, and then the decrease slows down. For the sample with 0.2 % graphene, the electrical resistivity drops more sharply (by 2 orders of magnitude) than for the sample with 0.5 % graphene (by 10 times). The sensitivity to deformation is higher for 7-day-cured samples compared to 14- and 28-day-cured ones. When the ultimate strength is reached, there is a sharp jump in electrical resistivity associated with sample failure. The behavior of the dependencies is similar for all curing times, indicating the reproducibility of the results. Thus, the introduction of graphene increases the sensitivity of concrete to compressive deformation. These graphs illustrate the possibility of using graphene-modified concrete as a self-sensing “smart” material.

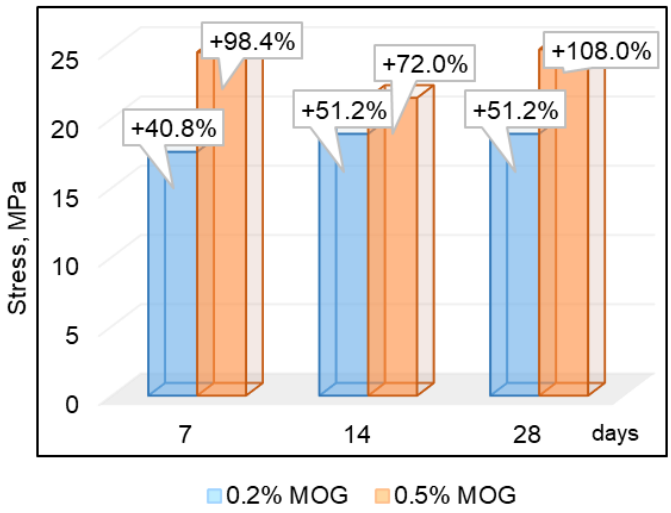

Figure 9. Graph of maximum breaking load for 7, 14, 28 days of curing of concrete samples modified with MOG.

4. Conclusion

1. The studies conducted using Raman and IR spectroscopy confirmed the successful incorporation of graphene nanoparticles into the inert mineral matrix of concrete. Structural distortions and various defects observed in graphene indicate its interaction with the cement composite components.
2. When MOG was added at 0.2 % of the cement weight, the resistivity decreased with increasing external load due to the compression of graphene sheets, which enhanced conductivity. The resistivity change rate decreased with further compression, and a sharp drop was noted at a certain load level, showing high sensitivity to mechanical deformation.
3. Concrete samples of grade M15 demonstrated a decrease in resistivity from the start of loading to 550–600 Ohm, returning to their initial values. The yield point was around 40–50 kN (plate pressure per 100 cm²). For cubic samples, increasing sensitivity to external loads required moistening. Measurements, taken both by the 2-probe method and with a digital multimeter, showed that moistened material could detect loads even with finger pressure (1 N).
4. The introduction of reduced oxidized graphene significantly improved the electrically conductive properties of concrete, offering broad application prospects:
   - Electromagnetic Shielding: Creates structures for protection against electromagnetic fields, useful in residential and industrial buildings [40, 41].
   - Self-Heating Concrete: Enables cost-effective heating for road surfaces, indoor floors, and prevents icing [42–48].
   - Sensory Structures: Detects mechanical stresses and deformations [49], aiding in structural integrity and operational optimization.
   - Corrosion Protection: Provides protection in reinforced concrete structures exposed to aggressive environments [50, 51].
   - Energy Storage: Enhances capacitive properties, paving the way for concrete batteries and supercapacitors [52, 53].

- Wireless Charging Roads: Facilitates the wireless charging of electric vehicles, increasing range and reducing charging time [54–56].

References

1. Krystek, M., Ciesielski, A., Samorì, P. Graphene-based cementitious composites: Towards next generation construction technologies. Advanced Functional Materials. 2021. 31(27). Pp. 2101887. DOI: 10.1002/adfm.202101887
2. Chung, D.D.L. Cement reinforced with short carbon fibers: a multifunctional material. Composites Part B: Engineering. 2000. 31(6–7). Pp. 511–526. DOI: 10.1016/S1359-8368(99)00071-2
3. Reddy, P., Ravi Prasad, D. Graphene oxide reinforced cement concrete - A study on mechanical, durability and microstructural characteristics. Fullerenes, nanotubes and carbon nanostructures. 2023. 31(3). Pp. 255-265. DOI: 10.1080/1536383X.2022.2141231
4. Suo, Y. et al. A Review of graphene oxide/cement composites: Performance, functionality, mechanisms and prospects. Journal of Building Engineering. 2022. 53. Pp. 104502. DOI: 10.1016/j.jobe.2022.104502
5. Sassani, A., Arabzadeh, A., Ceylan, H. et al. Carbon fiber-based electrically conductive concrete for salt-free deicing of pavements. Journal of Cleaner Production. 2018. 203. Pp. 799–809. DOI: 10.1016/j.jclepro.2018.08.315
6. Wang, X. et al. Mechanical and Electrical Properties of Multilayer Graphene Composite Conductive Concrete. Journal of Cold Regions Engineering. 2023. 37(3). Article no. 04023015. DOI: 10.1061/JCRGEI.CRENG-680
7. Arabzadeh, A. et al. Electrically conductive asphalt concrete: An alternative for automating the winter maintenance operations of transportation infrastructure. Composites Part B: Engineering. 2019. 173. Pp. 106985. DOI: 10.1016/j.compositesb.2019.106985
8. Choi, K., et al. Nanostructured thermoelectric composites for efficient energy harvesting in infrastructure construction applications. Ceramics International. 2022. 128. Pp. 104452. DOI: 10.1016/j.cemconcomp.2022.104452
9. Ghosh, S., Harish, S., Ohtaki, M., Saha, B.B. Enhanced figure of merit of cement composites with graphene and ZnO nanoinclusions for efficient energy harvesting in buildings. Energy. 2020. 198. Article no. 117396. DOI: 10.1016/j.energy.2020.117396
10. Kashif Ur Rehman, S. et al. A review of microscale, rheological, mechanical, thermoelectrical and piezoresistive properties of graphene based cement composite. Nanomaterials. 2020. 10(10). Pp. 2076. DOI: 10.3390/nano10102076
11. Rostami, H., Shao, Z., Boyd, M., He, Z. Mechanical properties of graphene oxide cement paste. Architecture, Civil Engineering, Environment. 2019. 12(1). Pp. 99–105. DOI: 10.21307/ACEE-2019-008
12. Jiang, S., Shang, Z., Hou, C. et al. Piezoresistive properties of ultra-high-performance fiber-reinforced concrete incorporating few-layer graphene. Construction and Building Materials. 2021. 305. Pp. 124362. DOI: 10.1016/j.conbuildmat.2021.124362
13. Pei, C., Ueda, T., Zhu, J. Investigation of the effectiveness of graphene/polyvinyl alcohol on the mechanical and electrical properties of cement composites. Materials and Structures. 2020. 53. Pp. 1-15.DOI: 10.1617/s11527-020-01508-6
14. Dimov, D. et al. Ultrahigh performance nanoengineered graphene–concrete composites for multifunctional applications. Advanced functional materials. 2018. 28(23). Pp. 1705183. DOI: 10.1002/adfm.201705183
15. Wang, S., Singh, A., Liu, Q. Experimental study on the piezoresistivity of concrete containing steel fibers, carbon black, and graphene. Frontiers in Materials. 2021. 8. Pp. 652614. DOI: 10.3389/fmats.2021.652614
16. Kedir, A., Gamachu, M., Alex, A. G. Cement-based graphene oxide composites: a review on their mechanical and microstructure properties. Journal of Nanomaterials. 2023. 2023(1). Pp. 6741000. DOI: 10.1155/2023/6741000
17. Li, W. et al. A comprehensive review on self-sensing graphene-cement composites: a pathway to next-generation smart concrete. Construction and Building Materials. 2022. 331. Pp. 127284. DOI: 10.1016/j.conbuildmat.2022.127284
18. Schulte J. et al. Graphene-reinforced cement composites for smart infrastructure systems. The Rise of Smart Cities. 2022. Pp. 79–114. DOI: 10.1016/B978-0-12-817784-6.00008-4
19. Chen, R. Preparation, property determination and bridge health monitoring applications of self-sensing cement nanocomposites. Alexandria Engineering Journal. 2023. 66. Pp. 891-900. DOI: 10.1016/j.aej.2022.10.061
20. Lu, D. et al. Growing nanocrystalline graphene on aggregates for conductive and strong smart cement composites. ACS nano. 2023. 17(4). Pp. 3587-3597. DOI: 10.1021/acsnano.2c10141
21. Polverino, S. et al. Few-layers graphene-based cement mortars: production process and mechanical properties //Sustainability. 2022. 14(2). Pp. 784. DOI: 10.3390/su14020784
22. Papanikolaou, I., Arena, N., Al-Tabbaa, A. Graphene nanoplatelet reinforced concrete for self-sensing structures–A lifecycle assessment perspective. Journal of Cleaner Production. 2019. 240. Pp. 118202. DOI: 10.1016/j.jclepro.2019.118202
23. Gokhale, D. G. K., Kaish, A. B. M. Recent trends in incorporating graphene coated sand in self-sensing cementitious composites. Materials Proceedings. 2023. 14(1). Pp. 48. DOI: 10.3390/IOCN2023-14544
24. Wang, Z., Wang, Z., Ning, M. et al. Electro-thermal properties and Seebeck effect of conductive mortar and its use in self-heating and self-sensing system. Ceramics International. 2017. 43(12). Pp. 8685–8693. DOI: 10.1016/j.ceramint.2017.03.202
25. Hu, Y. G. et al. Experimental study of the electrical resistance of graphene oxide-reinforced cement-based composites with notch or rebar. Journal of Building Engineering. 2022. 50. pp. 104331. DOI: 10.1016/j.jobe.2022.104331
26. Lavagna, L. et al. Cement-based composites containing oxidized graphene nanoplatelets: effects on the mechanical and electrical properties. Nanomaterials. 2023. 13(5). Pp. 901. DOI: 10.3390/nano13050901
27. Papanikolaou, I., Al-Tabbaa, A., Goisis, M. An Industry Survey on the Use of Graphene-Reinforced Concrete for Self-Sensing Applications. International Conference on Smart Infrastructure and Construction 2019 (ICSIC): Driving data-informed decision-making. ICE Publishing, 2019. Pp. 613–622. DOI: 10.1680/icsic.64669.613
28. Syama, S., Mohanan, P.V. Safety and biocompatibility of graphene: A new generation nanomaterial for biomedical application. International Journal of Biological Macromolecules. 2016. 86. Pp. 546–555. DOI: 10.1016/j.ijbiomac.2016.01.116
29. Xia L., Zhou M., Ni T., Liu, Z. Synthesis and characterization of a novel early strength polycarboxylate superplasticizer and its performances in cementitious system. Journal of Applied Polymer Science. 2020. 137(30). Article no. 48906. DOI: 10.1002/app.48906
30. Sobczyk-Guzenda, A. et al. Micro-and Nanoparticulate Hydroxyapatite Powders as Fillers in Polyacrylate Bone Cement – A Comparative Study. Materials. 2020. 13(12). Article no. 2736. DOI: 10.3390/ma13122736
31. Pang, B. et al. Ultraductile cementitious structural health monitoring coating: waterborne polymer biomimetic muscle polyhedral oligomeric silsesquioxane-assisted c-s-h dispersion. Advanced Functional Materials. 2022. 32(51). Article no. 2208676. DOI: 10.1002/adfm.202208676

32. Leonovich, S.N., Sadovskaya, E.A. Strength Indicators of Fiber Reinforced Concrete with Carbon Nanomaterials. Science & Technique. 2024. 23(3). Pp. 219–224. DOI: 10.21122/2227-1031-2024-23-3-219-224
33. Malakar, A. et al Mussel-inspired double cross-linked interpenetrating network with unique mechanical properties using di-diol complexation. SPE Polymers. 2023. 4(3). Pp. 83–92. DOI: 10.1002/pls2.10088
34. Shen, T., Wang, T., Qin, C., Jiao, N. Silver-catalyzed nitrogenation of alkynes: a direct approach to nitriles through C≡ C bond cleavage. Angewandte chemie international edition. 2013. 125(26). Article no. 6677–6680. DOI: 10.1002/anie.201300193
35. Bai, T., Li, H. Revealing the Mechanism of Alcohol Dehydroxylation and C–C Bond Formation through Concerted Catalysis by Ir/Cu Bimetallic Complexes. The Journal of Organic Chemistry. 2024. 89(8). Pp. 5363–5370. DOI: 10.1021/acs.joc.3c02740
36. Iranifam, M. MOFs-, COFs-and MOGs-assisted chemiluminescence methods. Microchemical Journal. 2024. 199. Article no. 110096. DOI: 10.1016/j.microc.2024.110096
37. Beskopylny, A.N., Shcherban', E.M., Stel'makh, S.A., Mailyan, L.R., Meskhi, B., Razveeva, I., Kozhakin, A., Beskopylny, N., El'shaeva, D., Artamonov, S. Method for Concrete Structure Analysis by Microscopy of Hardened Cement Paste and Crack Segmentation Using a Convolutional Neural Network. Journal of Composites Science. 2023. 7(8). Article no. 327. DOI: 10.3390/jcs7080327
38. Peng, H., Ge, Y., Cai, C. S., Zhang, Y., Liu, Z. Mechanical properties and microstructure of graphene oxide cement-based composites. Construction and Building Materials. 2019. 194. Pp. 102–109. DOI: 10.1016/j.conbuildmat.2018.10.234
39. Zhang, N., She, W., Du, F., Xu, K. Experimental Study on Mechanical and Functional Properties of Reduced Graphene Oxide/Cement Composites. Materials. 2020. 13(13). Article no. 3015. DOI: 10.3390/ma13133015
40. Khalid, T., Albasha, L., Qaddoumi, N.N., Yehia, S. Feasibility Study of Using Electrically Conductive Concrete for Electromagnetic Shielding Applications as a Substitute for Carbon-Laced Polyurethane Absorbers in Anechoic Chambers. IEEE Transactions on Antennas and Propagation. 2017. 65(5). Pp. 2428–2435. DOI: 10.1109/TAP.2017.2670538
41. Yehia, S., Qaddoumi, N.N., Hassan, M.S., Swaked, B. Conductive Concrete for Electromagnetic Shielding Applications. Advances in Civil Engineering Materials. 2014. 3(1). Article no. ACEM20130107. DOI: 10.1520/ACEM20130107
42. Wang, X. et al. Road use and electrothermal performance of graphene-conductive asphalt-recycled pervious concrete under severe cold environment. Construction and Building Materials. 2023. 400. Article no. 132829. DOI: 10.1016/j.conbuildmat.2023.132829
43. Maleki, P., Iranpour, B., Shafabakhsh, G. Investigation of de-icing of roads with conductive concrete pavement containing carbon fibre-reinforced polymer (CFRP). International Journal of Pavement Engineering. 2019. 20(6). Pp. 682–690. DOI: 10.1080/10298436.2017.1326235
44. Mingqing, S. et al. Experimental studies on the indoor electrical floor heating system with carbon black mortar slabs. Energy and Buildings. 2008. 40(6). Pp. 1094–1100. DOI: 10.1016/j.enbuild.2007.10.009
45. Yinfei, D. et al. Using silicon carbide to increase thermal conductivity of cement composite for improving heating efficiency of floor heating system. Construction and Building Materials. 2022. 325. Article no. 126707. DOI: 10.1016/j.conbuildmat.2022.126707
46. Heinlein, U., Freimann, T. Industrial concrete floors: evaluation of electrostatic dissipative properties according to IEC 61340-4-1. Construction and Building Materials. 2022. 329. Article no. 127162. DOI: 10.1016/j.conbuildmat.2022.127162
47. Lee, H., Yu, W., Loh, K.J., Chung, W. Self-heating and electrical performance of carbon nanotube-enhanced cement composites. Construction and Building Materials. 2020. 250. Article no. 118838. DOI: 10.1016/j.conbuildmat.2020.118838
48. Farcas, C. et al. Heating and de-icing function in conductive concrete and cement paste with the hybrid addition of carbon nanotubes and graphite products. Smart Materials and Structures. 2021. 30. Article no. 045010. DOI: 10.1088/1361-665X/abe032
49. Qin, H. et al. Revolutionizing infrastructure: The evolving landscape of electricity-based multifunctional concrete from concept to practice. Progress in Materials Science. 2024. 145. Article no. 101310. DOI: 10.1016/j.pmatsci.2024.101310
50. Sharma, N. et al. Evaluation of corrosion inhibition capability of graphene modified epoxy coatings on reinforcing bars in concrete. Construction and Building Materials. 2022. 322. Article no. 126495. DOI: 10.1016/j.conbuildmat.2022.126495
51. Sohn, H. et.al. Operation of battery-less and wireless sensor using magnetic resonance based wireless power transfer through concrete. Smart Structures and Systems. 2016. 17(4). Pp. 613–646. DOI: 10.12989/SSS.2016.17.4.631
52. Tian, Z. et al. Analysis and Optimization of Asymmetric Wireless Power Transfer in Concrete. Wireless Communications and Mobile Computing. 2020. 2020(1). Article no. 8841210. DOI: 10.1155/2020/8841210
53. Basha, S.I. et al. Construction building materials as a potential for structural supercapacitor applications. The Chemical Record. 2022. 22(11). Article no. e202200134. DOI: 10.1002/tcr.202200134
54. Nguyen, D.H. Dynamic optical wireless power transfer for electric vehicles. IEEE Access. 2023. 11. Pp. 2787–2795. DOI: 10.1109/ACCESS.2023.3234577
55. Behnamfar, M., Tariq, M., Sarwat, A. Novel combined inductive and capacitive wireless power transfer system to reduce power pulsation for dynamic charging of electric vehicles. 2023 IEEE Industry applications society annual meeting (IAS), Nashville, 2023. Pp. 1–6. DOI: 10.1109/IAS54024.2023.10406764
56. Yang, L. et al. Differentiated speed planning for connected and automated electric vehicles at signalized intersections considering dynamic wireless power transfer. Journal of Advanced Transportation. 2022. Article no. 5879568. DOI: 10.1155/2022/5879568

Information about the authors:

Elena Vasileva,
ORCID: https://orcid.org/0000-0001-8953-9309
E-mail: vasilyeva_edm@mail.ru

Dmitry Popov,
ORCID: https://orcid.org/0000-0001-9639-7601
E-mail: dmiitryy09@gmail.com

Pavel Vinokurov,
ORCID: https://orcid.org/0000-0003-2004-6631
E-mail: pv.vinokurov@s-vfu.ru

Aleksandr Popov, *PhD in Technical Scieneces*
ORCID: https://orcid.org/0000-0002-7829-6839
E-mail: surrukin@gmail.com

Received 25.01.2024. Approved after reviewing 26.11.2024. Accepted 30.11.2024.